
EFDA–JET–CP(01)02-65

K. Borrass, R. Monk, W. Suttrop, J. Schweinzer, J. Rapp, J. Ongena,
G. Saibene, L. Horton, V. Mertens and JET EFDA Contributors

Recent H-Mode Density Limit Studies on JET

Recent H-Mode Density Limit Studies on JET

K.Borrass¹, R.Monk¹, W.Suttrop¹, J.Schweinzer², J.Rapp³, J.Ongena⁴,
G.Saibene⁵, L.Horton¹, V.Mertens¹ and JET EFDA Contributors*

¹*Max-Planck-Institut für Plasmaphysik, Euratom Association, Garching, Germany*

²*EFDA Close Support Unit, Culham, United Kingdom*

³*Institut für Plasmaphysik, Forschungszentrum Jülich, Euratom Association, Jülich, Germany*

⁴*Laboratoire de Physique des Plasmas, École Royale Militaire, Euratom Association, Brussels, Belgium*

⁵*EFDA Close Support Unit Garching, Garching, Germany*

**See appendix of the paper by J.Pamela "Overview of recent JET results",
Proceedings of the IAEA conference on Fusion Energy, Sorrento 2000*

Preprint of Paper to be submitted for publication in Proceedings of the
EPS Conference,
(Madeira, Portugal 18-22 June 2001)

“This document is intended for publication in the open literature. It is made available on the understanding that it may not be further circulated and extracts or references may not be published prior to publication of the original when applicable, or without the consent of the Publications Officer, EFDA, Culham Science Centre, Abingdon, Oxon, OX14 3DB, UK.”

“Enquiries about Copyright and reproduction should be addressed to the Publications Officer, EFDA, Culham Science Centre, Abingdon, Oxon, OX14 3DB, UK.”

ABSTRACT

Recent studies on ASDEX Upgrade have revealed differences between the empirical H-mode density limit scaling and the widely used Greenwald scaling, particularly as regards the B_t and q_ψ dependences. Dedicated low B_t and high q_ψ gas scans have been performed at JET to address this issue. A combined JET and ASDEX Upgrade database is analyzed and is found to be described by a common scaling which confirms the expected deviations from the Greenwald scaling. A comparison of the empirical scaling with model predictions is made and its implications for the critical density of ITER are discussed. The paper also includes a discussion of the JET density limit signatures with a view to resolving apparent differences between JET and smaller tokamaks. A coherent inter machine picture, underlying the present paper, is obtained if the density limit is conceived as a limit of the pedestal density that is reached at the H-L transition boundary.

INTRODUCTION

Traditionally the concept of a density limit (DL) is applied to the highest density achieved in a system which is actively fed with particles (density ramp-up). DLs can be attributed to specific tokamak operation regimes (L-mode DL, H-mode DL). Furthermore, the highest density may be achieved at the high density boundary of the operation regime so that the density limit coincides with a regime transition (H to L transition H-mode DL, disruptive L-mode DL) or it may manifest itself as a resilience to further density increase (soft density limit). Finally the limit can be formulated as a limit for certain moments of the density profile (line average, volume average) or for values taken at certain radial position (pedestal, separatrix). Here the particular choice is typically determined by the requirement of a simple and coherent description of empirical data and/or ideas about the underlying physics or, sometimes, simply by limitations of the available diagnostics. Historically the disruptive L-mode density limit and the H-L transition H-mode density limit have been the main focus, but the definitions are general enough to include also recent extensions of the concept such as the Type-I ELM H-mode DL [1].

In medium size tokamaks the line average density \bar{n} and the pedestal density n_{ped} monotonically increase in a density ramp-up and reach their maximum values at the (high density) H-L transition boundary, thus making the definition of a DL obvious [2]. JET high density scans differ in several respects: while n_{ped} normally increases monotonically in a gas scan, n typically saturates or even goes through a weak maximum. Also, operational limitations (beam duct overpressure trips) make it difficult to reach the H-L transition boundary in a wide parameter range. All this makes the proper definition of a DL less obvious. In order to study these apparent differences in greater detail, a series of dedicated gas scan were recently performed in a parameter range where the H-L boundary can be reliably reached. Details of these scans are discussed in Sec. 2 with a view to a proper DL definition and a coherent inter machine picture.

The JET database is relatively scarce in the low B_t and high q_ψ range and therefore these runs were performed in this range. Scaling information on B_t and q_ψ is of particular interest, since various proposed DL models differ mainly in their predicted B_t and q_ψ dependencies. Finally, B_t is significantly higher in ITER than in current tokamaks, making knowledge of the B_t dependence mandatory for a reliable extrapolation. The same is true of the size dependence. We therefore combine the extended JET database with the ASDEX Upgrade database of Ref. [2], to derive an experimental scaling covering all relevant variables (Sec. 3).

2. JET DENSITY RAMP-UP SIGNATURES

In JET, density ramp-ups are typically realized by performing a sequence of discharges with constant, but successively increasing gas rates. (In this study we confine ourselves to gas fuelled discharges.) In Fig.1 the evolution of line averaged and pedestal densities are shown for a recent mediumed, medium current gas box divertor scan. It is typical in that \bar{n} saturates and eventually shows a mild drop, (normally not exceeding 10%), while n_{ped} increases monotonically until the H-L boundary is reached. The non monotonic relation between \bar{n} and n_{ped} is due to profile flattening as is illustrated in Fig.2. This suggests defining the H-mode density limit as a limit of the edge (pedestal) density which is reached at the high density H-L transition boundary. Apart from the decrease of the density peaking toward complete flatness a further generally observed feature of this limit is a drop of the inter-ELM I_{sat} by typically one order of magnitude [3], this being indicative of divertor detachment between ELMs [4]. Thus, by adopting this DL definition one obtains a picture for the H-mode DL in JET which is in line with findings on ASDEX Upgrade [2]. The only difference, namely the non-monotonic behaviour of \bar{n} , is naturally attributed to differences in core peaking which are likely to be governed by core physics.

3. SCALING OF THE DENSITY LIMIT

The \bar{n} evolution in a JET gas scan shows, in agreement with the example of Sec. 2, the following pattern: \bar{n} saturates, goes through a plateau and finally drops slightly ($\approx 10\%$) when the limit is approached. A sizeable fraction of JET high density gas scans reach the plateau, but, due to operational constraints, fail to reach the high density H-L boundary (“incomplete scans”). In the light of the smallness of the drop in the final phase and the flatness of the density profile at the limit, we have, however, with acceptable accuracy $\bar{n}_{plateau} \sim \bar{n}_{DL} \sim n_{ped,DL} \equiv n_{DL}$, where subscript $_{DL}$ indicates values at the DL proper and the meaning of the other notations is obvious. This allows us to include incomplete scans into our database by identifying n_{DL} with $\bar{n}_{plateau}$. With this rule applied, our database comprises discharges from the JET Mark-I, Mark-II and gas box divertor configurations. All discharges are beam heated and the majority have low triangularity.

In order to get information on the size dependence of the DL, we include data obtained in the ASDEX Upgrade Divertor II configuration in our analysis. A detailed discussion of these data and an in-depth analysis, much along the lines of this paper, has been presented in Ref. [2].

Applying the usual assumptions of least-squares regression on this full set of JET and ASDEX Upgrade data we obtain the empirical scaling

$$n_{\text{DL, fit}} = 35.2 \frac{q_{\perp}^{0.052 \pm 0.034} B_t^{0.58 \pm 0.11}}{(q_{95} R)^{0.88 \pm 0.11}} \quad (1)$$

[10^{19}m^{-3} , MWm^{-2} , T, m], where $q_{\perp} = (P_{\text{heat}} - P_{\text{rad}}^{\text{tot}}) / S$ and S is the plasma surface. The exponents are given with their 95% confidence intervals. The particular parameter choice was guided by Ref. [5].

As discussed in Sec. 2, the achievement of the DL coincides with complete inter ELM divertor detachment. Thus, the model for the (pedestal) density $n_{\text{DL, BLS}}$ at complete detachment proposed by Borrass, Lingertat and Schneider [5] should describe our data. It results in the scaling (Eq. (7) of Ref. [5])

$$n_{\text{DL, BLS}} = 41.4 \frac{q_{\perp}^{0.09} B_t^{0.53}}{(q_{95} R)^{0.88}} \quad (2)$$

[10^{19}m^{-3} , MWm^{-2} , T, m], which is in remarkable agreement with Eq. (1).

It is also illuminating to compare our findings with the empirical Greenwald scaling which is widely used as a kind of reference scaling [6]:

$$n_{\text{DL, GW}} = \frac{I_p}{\pi a^2} \equiv 15.9g \frac{B_t}{q_{95} R} \quad (3)$$

[10^{19}m^{-3} , MA, T, m], where I_p is the plasma current, a is the plasma minor radius. The factor $g = q_{95} = q_c$ ($q_c = \frac{2\pi}{2} \frac{a^2 B_t}{RI_p}$ the cylindrical q) is determined by the plasma shape (elongation, triangularity), basically kept constant in our database.

The quality of the various models is visualized in Fig.3. The empirical scaling and the BLS scaling are hardly distinguishable (Figs.3(a) and (b)). The Greenwald densities are in the right absolute range, but the overall fit is rather poor (Fig.3(c)).

Much of the discrepancy between the Greenwald scaling and our results from the different B_t dependence in Eqs (1) and (3). Therefore, in a machine like ITER [7] with its much higher field the difference would be rather pronounced and the critical (pedestal) density according to Eqs (1) or (2) would be about 40% below the Greenwald value. At present it is difficult to decide precisely what this means for the operation of a reactor grade plasma. When the H-L boundary is approached, confinement degrades and ITER will have to operate at densities sufficiently below this limit to achieve acceptable confinement, presumably close to the Type I to Type III boundary. Thus, the H-mode density limit sets an upper limit on the pedestal density at the actual operation point. It has to be met simultaneously with requirements on the line average density. Currently density peaking is considered as an option to bring these constraints together. Any decrease of the predicted maximum pedestal density raises the demand on peaking necessary to meet the requirements on the line

average density. In that sense one consequence of our findings is that stronger peaking is needed in ITER than in current machines to achieve a certain “Greenwald fraction” of \bar{n} . However, the present analysis is basically confined to low triangularity discharges and the effect of triangularity on the H-mode density limit remains to be assessed. High triangularity H-mode density limit studies are planned at JET and ASDEX Upgrade.

REFERENCES

- [1]. A.V.Chankin, G.Saibene, Plasma Phys. Control. Fusion 41 (1999) 913.
- [2]. V.Mertens, K.Borrass, J.Gafert, et al., Nuclear Fusion 40 (2000) 1839.
- [3]. K.Borrass, et al., in preparation.
- [4]. K.Borrass, D.Coster, D.Reiter, R.Schneider, J. Nucl. Mater 241-243 (1997) 250.
- [5]. K.Borrass, J.Lingertat, R.Schneider, Contrib. Plasma Phys. 38 (1998) 130.
- [6]. M.Greenwald, et al., Nucl. Fusion 28 (1988) 2199.
- [7]. ITER Physics Basis Editors, ITER Physics Expert Group Chairs and Co-Chairs, ITER Joint Central Team and Physics Integration Unit, Nucl. Fusion 39 (1999) 2137.

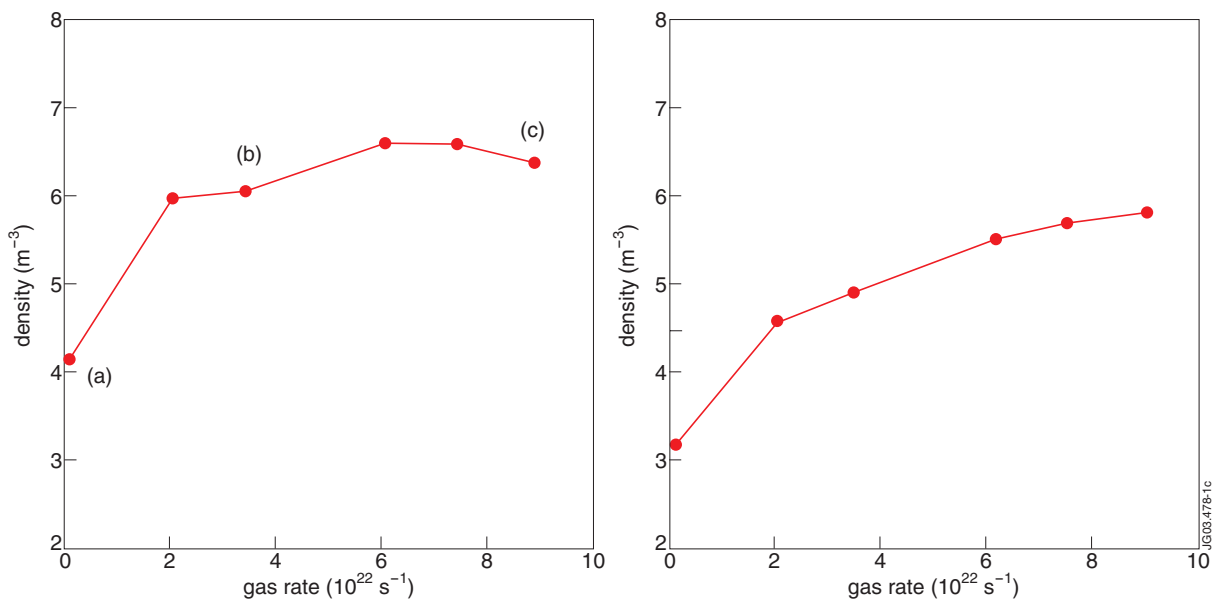


Figure 1: Line averaged density (left hand side) and pedestal density at $R = 3.7\text{m}$ (right hand side) versus gas rate in a mediumeld ($B_t = 1.9\text{T}$), medium power ($P_h = 8\text{MW}$), medium q_{95} ($q_{95} = 2.9$) gas scan (Lidar).

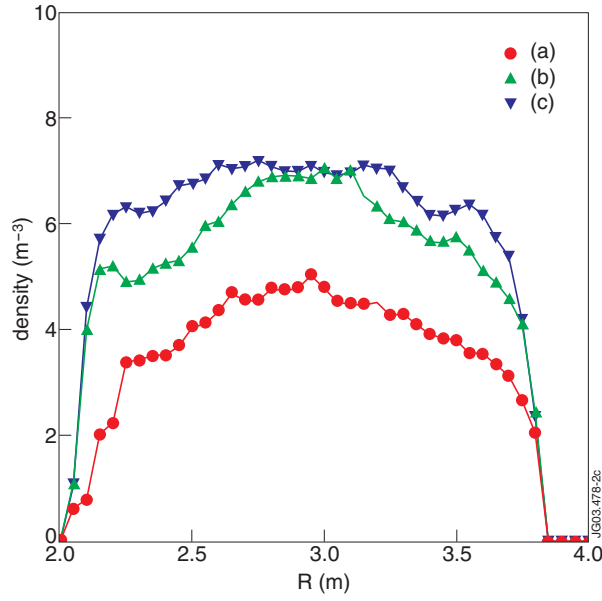


Figure 2: Electron density profiles (Lidar) at various points of the gas scan of Fig. 1. Profiles a) to c) correspond to stages a) to c) of Fig. 1. Each profile is the average of three adjacent profiles which were taken in between ELMs.

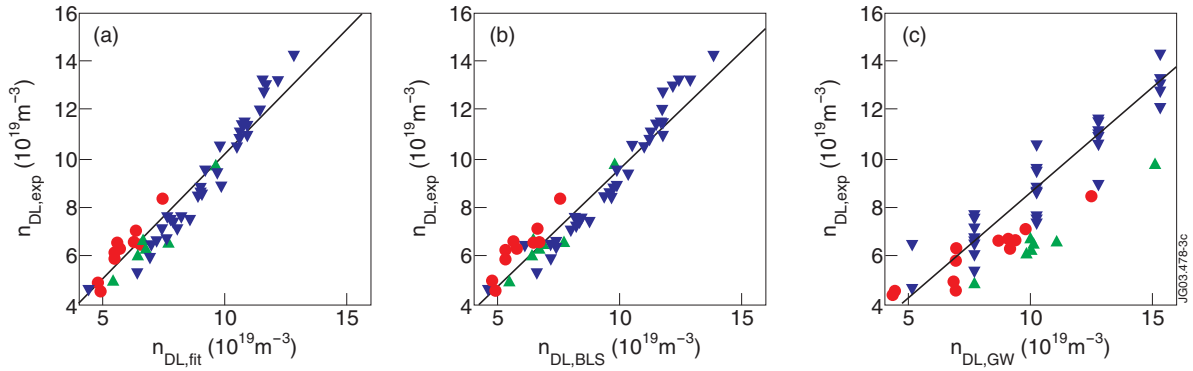


Figure 3: Experimental density limit $n_{DL,exp}$ (Lidar) versus $n_{DL,fit}$ (a), $n_{DL,BLS}$ (b) and Greenwald density $n_{DL,GW}$ (c). Experimental data are from JET Mark-I and Mark-II (upward triangles), the gas box divertor coniguration (bullets) and from the ASDEX Upgrade Divertor II coniguration (downward triangles). Within the database the variations of P_{pl} , B_1 and q_{95} cover the ranges 3.5-19.5MW, 1.0-3.5T and 2.5-11.5, respectively.